

## Original Article

## LTE physical layer: Performance analysis and evaluation

H. Mousavi <sup>a</sup>, Iraj S. Amiri <sup>b,c\*</sup>, M.A. Mostafavi <sup>a</sup>, C.Y. Choon <sup>a</sup><sup>a</sup> Department of Electrical and Telecom, Faculty of Engineering, Multimedia University, Cyberjaya, Selangor, Malaysia<sup>b</sup> Computational Optics Research Group, Ton Duc Thang University, Ho Chi Minh City, Viet Nam<sup>c</sup> Faculty of Applied Sciences, Ton Duc Thang University, Ho Chi Minh City, Viet Nam

## ARTICLE INFO

## Article history:

Received 10 June 2017

Accepted 19 September 2017

Available online 27 September 2017

## Keywords:

LTE  
Performance evaluation  
SISO  
MIMO

## ABSTRACT

3GPP LTE was proposed by cooperation between groups of telecommunications consortium named as 3rd Generation Partnership Project to improve the Universal Mobile Telecommunications System (UMTS) standard. It supports up to 300 Mbps of data transmission in downlink using the Orthogonal Frequency Division Multiplexing (OFDM) modulation as well as up to 75 Mbps throughput for uplink using the Single Carrier-Frequency Division Multiple Access (SC-FDMA) modulation schemes. In this paper, the study of LTE PHY layer performance evaluation is conducted for downlink transmission utilizing Single-Input and Single-Output (SISO) and Multi-Input and Multi-Output (MIMO) techniques. We present a comprehensive investigation of the LTE performance analysis, where the Bit Error Rate (BER), Block Error Rate (BLER) and throughput performance results of LTE PHY layer provided.

© 2017 The Authors. Production and hosting by Elsevier B.V. on behalf of King Saud University. This is an open access article under the CC BY-NC-ND license (<http://creativecommons.org/licenses/by-nc-nd/4.0/>).

## 1. Introduction

Providing higher-speed data transmission has always been the most concerned objective of the 4th generation of mobile communication standards. That is why these standards have constantly been suffering from prohibitive cost, splintering of technology standards and lack of user interest. Evolved UMTS Terrestrial Radio Access Network (E-UTRAN) is one of the 4th generation mobile communication standards for mobile communications introduced by 3rd Generation Partnership Project (3GPP) [1]. Unlike 3rd generation standards which use CDMA technique, LTE makes use of Orthogonal Frequency Division Multiplexing (OFDM) for downlink and Single Carrier-Frequency Division Multiple Access (SC-FDMA) for uplink transmission. It has a very flexible radio interface, and its core network is called System Architecture Evolution (SAE) or Evolved Packet Core (EPC). The most serious rival for LTE standard is the IEEE 802.16e standard, which is well-known as WiMAX and was developed by IEEE [2,3].

## 2. Overview of 3GPP LTE

## 2.1. System architecture

LTE came up with a new network architecture called SAE. SAE architecture consists of two main parts: EPC and E-UTRAN (Fig. 1). These two parts together form a system called Evolved Packet System (EPS). EPS routes the IP packets with a given QoS, from Packet Data Network Gateway (P-GW) to User Equipment (UE). E-UTRAN manages the radio resources and makes sure of the security of transmitted data [4]. E-UTRAN entirely consists of base stations only, which are connected to the UEs providing network air interface roles. E-UTRAN architecture is flat, thus there is no centralized controlling in E-UTRAN [5]. E-UTRAN and EPC network components are connected together via standard interfaces [6].

The EPC enables commuting data packets with the internet as well as UE while a given QoS is maintained. EPC includes Home Subscriber Service (HSS), Policy Control and Charging Rules Function (PCRF), Mobility Management Entity (MME), P-GW and Serving Gateway (S-GW).

## 2.2. Protocol architecture of LTE physical layer

Fig. 2 illustrates the physical layer protocol architecture between LTE network and UE. This air interface is composed of three layers commonly called layers 1, 2 and 3. The medium access control (MAC) layer transport channels, in the upper levels, are

\* Corresponding author at: Ton Duc Thang University, Ho Chi Minh City, Viet Nam.

E-mail address: [irajsadeghamiri@tdt.edu.vn](mailto:irajsadeghamiri@tdt.edu.vn) (I.S. Amiri).

Peer review under responsibility of King Saud University.



Production and hosting by Elsevier

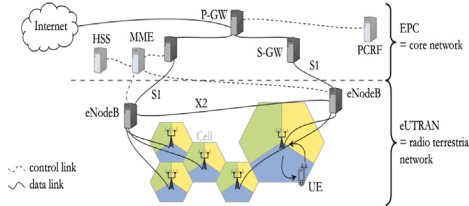


**Fig. 1.** LTE System Architecture Evolution [7].

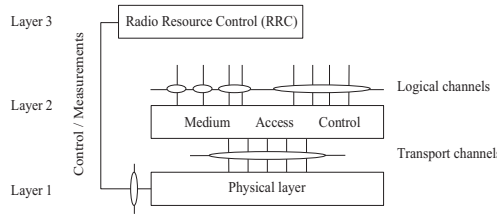


**Fig. 2.** Protocol architecture around the LTE PHY layer [8].

connected to logical channels which link the MAC layer to the RLC layer.

The logical channels in the MAC layer are characterized by the type of data transferred through them.

### 2.3. Multiple access techniques

The downlink transmission utilizes a multiple access scheme based on OFDM with a Cyclic Prefix (CP) while the uplink transmission uses a scheme based on SC-FDMA with a CP [9]. Since OFDM allows us to avoid Inter-Symbol Interference (ISI), transmission of high-speed serial streams is highly possible. The LTE supports transmission on a dedicated carrier for Multicast/Broadcast over a Single Frequency Network (MBSFN) [10,11] by utilizing a longer CP with a subcarrier spacing of 7.5 kHz. MIMO techniques are employed in LTE [12]. LTE also maintains aggregation of multiple cells in both uplink and downlink directions with up to five serving cells, where each serving cell can have a transmission bandwidth of up to 20 MHz.

### 2.4. Physical resource allocations

The LTE physical layer supports two types of frame structures as types 1 and 2. The type 1 structure (Fig. 3) is used for Frequency Division Duplex (FDD) mode; however, the type 2 structure (Fig. 4) is applied to Time Division Duplex (TDD) mode maintaining only full duplex operation. Type 1 lasts 10 ms equivalent to 10 subframes (each 1 ms long) or 20 slots (each 0.5 ms long). As in FDD, each frame consists of 10 subframes of 1 ms long and each subframe consists of two concatenated slots of 0.5 ms long. The radio frame used in TDD mode (type 2) also has a length of 10 ms, but it is divided to two half-frames of length 5 ms. Just like the FDD, each subframe of type 2 frame structure also consists of two slots of length 0.5 ms. The special subframe in each half-frame includes

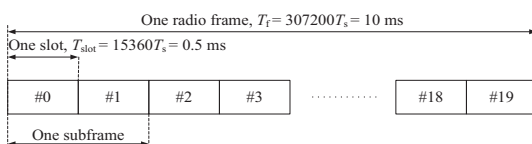


**Fig. 3.** Frame structure type 1 [13].

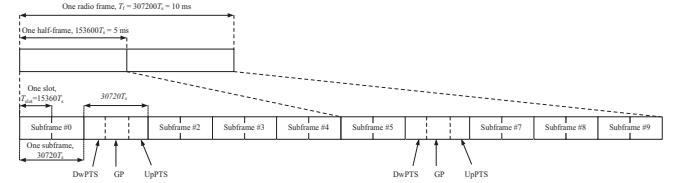


**Fig. 4.** Frame structure type 2 [13].

three fields; DwPTS (Downlink Pilot Time Slot), GP (Guard Period) and UpPTS (Uplink Pilot Time Slot).

The transmitted signal within each slot is defined by a resource grid of  $N_{\text{RB}}^{\text{UL}} N_{\text{sc}}^{\text{RB}}$  subcarriers and  $N_{\text{Symb}}^{\text{UL}}$  SC-FDMA symbols for uplink, and a resource grid of  $N_{\text{RB}}^{\text{DL}} N_{\text{sc}}^{\text{RB}}$  subcarriers and  $N_{\text{Symb}}^{\text{DL}}$  OFDM symbols for downlink. Uplink and downlink resource grids are shown in Fig. 5 and Fig. 6 respectively.

The  $N_{\text{RB}}^{\text{UL}}$  parameter in the uplink transmission is based on the bandwidth set in cells and must satisfy the equation bellow.

$$N_{\text{RB}}^{\min, \text{UL}} \leq N_{\text{RB}}^{\text{UL}} \leq N_{\text{RB}}^{\max, \text{UL}} \quad (1)$$

Whereas, the value of  $N_{\text{RB}}^{\text{DL}}$  defined in downlink transmission varies based on the downlink bandwidth configured in cells and must satisfy the equation bellow.

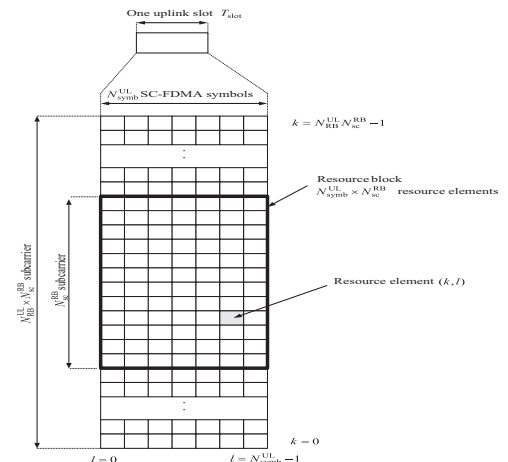


**Fig. 5.** Uplink resource grid [13].

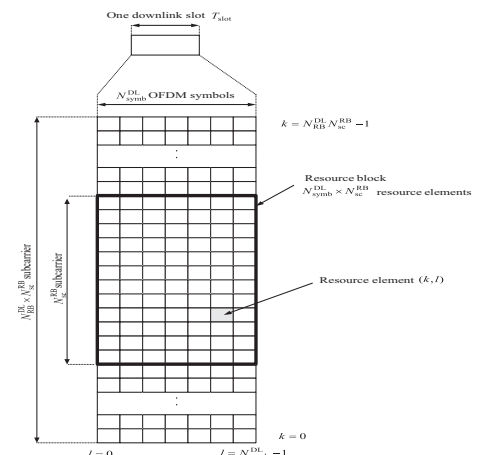


**Fig. 6.** Downlink resource grid [13].

**Table 1**

Resource Block Configurations [13].

CHANNEL	1.4	3	5	10	15	20
Number of RBs	6	15	25	50	75	100

**Table 2**

Resource Block Parameters.

		Normal	Extended Cyclic Prefix	
		Subcarrier Spacing: 15 kHz	Subcarrier Spacing: 15 kHz	Subcarrier Spacing: 7.5 kHz
Uplink	$N_{\text{symb}}^{\text{UL}}$	7	6	–
	$N_{\text{SC}}^{\text{RB}}$	12	12	–
Downlink	$N_{\text{symb}}^{\text{DL}}$	7	6	3
	$N_{\text{SC}}^{\text{RB}}$	12	12	24

**Table 3**

Physical Channels.

Physical Layer		Transmission
PBCH	Physical Broadcast Channel	Downlink
PMCH	Physical Multicast Channel	Downlink
PDCCH	Physical Downlink Control Channel	Downlink
PUCCH	Physical Uplink Control Channel	Uplink
PDSCH	Physical Downlink Share Control Channel	Downlink
PUSCH	Physical Uplink Share Control Channel	Uplink
PCFICH	Physical Control Format Indicator Channel	Downlink
PHICH	Physical Hybrid ARQ Indicator Channel	Downlink
PRACH	Physical Random Access Channel	Uplink

$$N_{\text{RB}}^{\text{min},\text{DL}} \leq N_{\text{RB}}^{\text{DL}} \leq N_{\text{RB}}^{\text{max},\text{DL}} \quad (2)$$

The minimum and a maximum number of resource blocks for both uplink and downlink are 6 and 100 respectively. Table 1 shows the resource block (RB) configuration for different channel bandwidths.

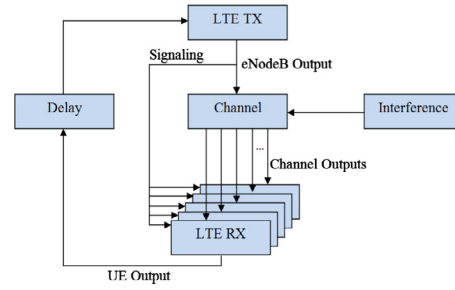
The number of symbols (SC-FDMA symbol in uplink and OFDMA symbols in downlink direction) per slot is configured based on the CP length and the subcarrier spacing selected by the higher layers. The small blocks in the resource grids are Resource Elements (RE), and a set of REs forms an RB. Hence, the number of REs existed in each RB is  $N_{\text{symb}}^{\text{UL}} \times N_{\text{sc}}^{\text{RB}}$  for uplink, and  $N_{\text{symb}}^{\text{DL}} \times N_{\text{sc}}^{\text{RB}}$  for downlink transmission, which in fact spans 180 kHz in the frequency domain and one 0.5 ms in the time domain. Table 2 presents the Resource Blocks parameters for both uplink and downlink.

The physical channels listed in Table 3 have specific tasks to accomplish to have successful uplink/downlink data transmissions.

### 3. Performance evaluation Of LTE physical layer

#### 3.1. Link level simulator

We have utilized only the Link Level simulation (Fig. 7) for downlink transmissions [13–15]. In LTE, the transmission process starts when user data is generated and tailed with Cyclic Redundancy Check (CRC) [16]. In next step, each user's data is encoded independently using a turbo encoder. Then each coded block is interleaved and rate-matched to achieve the target rate, and then modulated based on the received Channel Quality Indicator (CQI) feedback value [17]. The possible modulation schemes are 4-QAM, 16-QAM, and 64QAM.

**Fig. 7.** LTE link level simulator structure [15].

The User Equipment absorbs the signal transmitted by the evolved Node Base (eNodeB) and performs the reverse processing made by the transmitter. The receiver in UE then provides the necessary information (Fig. 7).

#### 3.2. LTE physical layer modulation

Adaptive modulation and coding, support of MIMO systems and HARQ are the key features of the LTE downlink. The modulation schemes specified in [13] for downlink transmission are 16-QAM, 64-QAM, BPSK, and QPSK.

#### 3.3. LTE downlink physical channel processing

In LTE, data and control information are encoded down from the MAC to the physical layer and decoded back from physical to MAC layer to serve transport and control Channels. Once the channel coding is performed, its output will be kept in a circular buffer where Redundancy Versions (RVs) are constituted. An RV is considered as the retransmission unit in the Hybrid Automatic Repeat request (HARQ) technique, and maximum 4 of them are permitted to be used in LTE.

The signal processing is shown in Fig. 8. First, the coded bits in every codeword are scrambled and conveyed to physical channels. The next step is to map these complex-valued modulated symbols into one or few transferring layers. Once the layer mapping is done, the process of precoding of modulated symbols on each layer will be started and the output will be conveyed to the antenna ports. The precoded symbols for each antenna port are then mapped into resource elements, and eventually, generation of time-domain OFDM signal for every single antenna port takes place. At the UE, to detect the transmitted signal and discover the original data, a

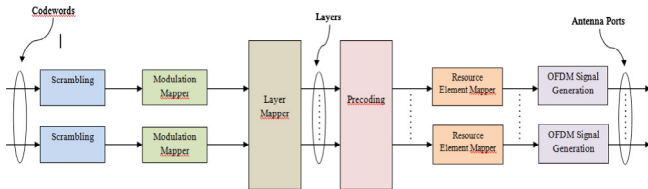


**Fig. 8.** Physical channel processing [13].

reverse procedure of transmitter is performed. The receiver must send requests for up to 3 retransmissions of redundancy version to the transmitter.

#### 3.4. Channel Coding, Interleaving and rate matching

The turbo encoder used in LTE consists of two convolutional concatenated encoders that are connected by an interleaver. The code rate of turbo coder used in the LTE is 1/3 and its two generated polynomials are  $G_0 = [1011]$  and  $G_1 = [1101]$ . From two candidates as Quadratic Permutation Polynomial (QPP) and Almost Regular Permutation (ARP), QPP was selected to improve the maximum throughput of the system. This interleaver is a conflict-free parallel turbo coder and provides maximum flexibility in supporting the parallelism. In LTE, the value for QPP inverse polynomial interleaver is 4. From the 1/3 rate output of the turbo coder, Rate Matching (RM) algorithm selects bits for transmission via puncturing or repeating. In rate matching, the bits in the code block are punctured and repeated to achieve a desired Effective Code Rate (ECR).

#### 4. Performance evaluation metrics

The LTE Link Level Simulator has key features such as the Adaptive Modulation and Coding (AMC). It consists of few functional sections, which are one eNodeB (transmitter), N number of UEs (receivers), a downlink channel model, signaling information, and an error-free uplink feedback channel with adjustable delay. A complete set of physical layer variables can be modified in the simulator. The eNodeB can estimate the code rate and modulation scheme by using the Sounding Reference Signal (SRS). Refs. [18–22] have presented the physical layer throughput as 100 Mbps, 150 Mbps and 300 Mbps for 1, 2 and 4 antenna ports respectively. Based on bandwidth of 1.4–20 MHz, the number of antenna ports (1, 2, or 4), the number of OFDM symbols assigned for PDCCH (1, 2, or 3 symbols per subframe), different channel code rates (0.0762–0.9258) and modulation schemes (4-QAM, 16-QAM, or 64-QAM), different system throughput performance as well as BER and BLER performances were obtained. The MIMO system models are described in detail in [23–26]. The input of this simulator is 500 subframes with random transmitting data selected by the simulator itself. For the results of this downlink simulation, average values of throughput, BER, and BLER vs. average values of SNR are calculated and plotted in form of MATLAB figures.

#### 5. Results and discussion

##### 5.1. Simulation parameters

Besides PDSCH, there are other physical channels (e.g. PBCH, PDCCH, and PMCH); however, this information is mainly control and broadcast information. **Table 4** summarizes the simulation parameters and depicts those configured for the simulation work.

**Table 4**  
Simulation parameters.

Parameter	Value (s)
Channel Bandwidth	1, 4, 3, 5, 10 MHz
Channel Type	AWGN, PedB, VehB, Flat Rayleigh
FEC Coding Scheme	Turbo Coding, Rate = 1/3
Modulation Scheme	4-QAM, 16-QAM, 64-QAM
Frame Period	10 ms
Subcarrier Spacing	15 kHz
Cyclic Prefix	Normal
Code Rate	0.0762 to 0.9258
Antenna Diversity	SISO, MIMO 2 × 1, MIMO 2 × 2, MIMO 4 × 2, OLSM 4 × 2
Number of Turbo Code Iterations	1, 3, 5, 8, 15, 20
Number of CQI feedbacks	1, 3, 6, 7, 9, 10, 12, 15
Number of HARQ retransmissions	No HARQ, 3 HARQ
Channel Estimators	Perfect, LS, MMSE
Maximum User Speed	100 km/h
Number of Subframes	500

We have considered stable user equipment's, channel bandwidth of 1.4 MHz, channel type of AWGN with the ideal channel estimator (Perfect), CQI = 9, 8 turbo code iterations, and 3 HARQ retransmissions for simulation.

##### 5.2. SISO techniques

SISO or Single-Input and Single-Output technique is a wireless communications system in which the only one transmit antenna is used at the transmitter and only one receive antenna is used at the receiver to carry out the transmission.

###### 5.2.1. Performance analysis of different CQI numbers

In Fig. 9 the BER curves for different CQI feedback values and modulation schemes are presented under different channel conditions (Channel SNR). It can be seen from the figure that for channel SNR values lower than  $-5$  dB, the CQI = 1, which used 4-QAM modulation scheme and ECR of 0.0762, has the lowest error rate, thus the best transmission quality. Lower order modulation schemes have lower data rates as the number of bits per symbol is less. It results in increasing the symbol pulse-width thus decreasing signal bandwidth and a better BER performance.

However, in the case of increasing channel SNR, CQI = 9, which utilizes 16-QAM modulation scheme and ECR = 0.6016 appears to

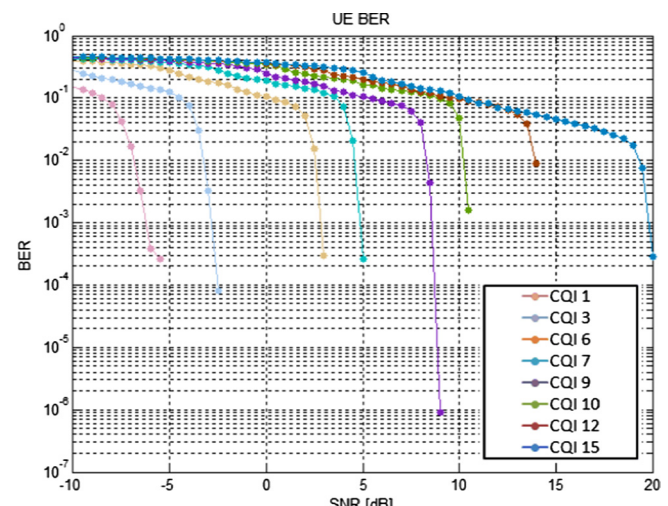


**Fig. 9.** BER vs. SNR for different CQI Values, SISO.

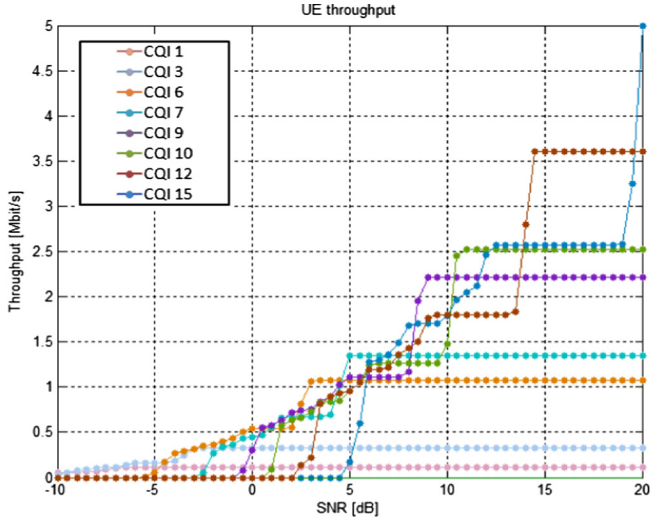


Fig. 10. Throughput vs. SNR for different CQI values, SISO.

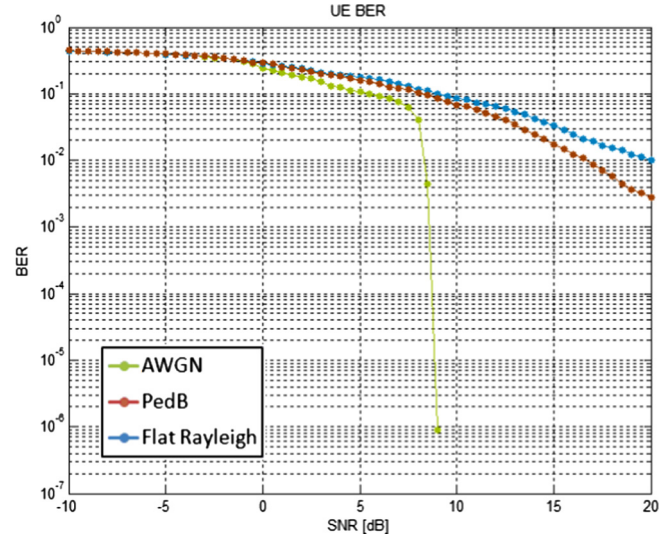


Fig. 11. BER vs. SNR for different channel types, SISO.

be the most efficient CQI feedback value for downlink transmission as it results in BER improvement until  $\text{BER} = 10^{-6}$  at a desirable channel SNR of 8 dB. This is because of using very effective error protection level ( $\text{ECR} = 0.6016$ ) associated with the modulation scheme for this CQI feedback. Decreasing of the error rate is performed by applying a better ECR and a better Cyclic Redundancy Check (CRC) scheme. Table 5 shows the CQI user feedback configuration of the LTE downlink simulator.

### 5.2.2. Performance analysis of different channel types

In Fig. 11, the BER performance of AWGN, Pedestrian B (PedB) and Flat Rayleigh, is investigated. In terms of error rate, the AWGN channel provides the lowest error at low channel SNR values, as the  $\text{BER} = 10^{-6}$  is achieved at the channel SNR = 8 dB. However, PedB and Flat Rayleigh channel models result in poorer BER performances in comparison with AWGN. The PedB channel results in a better BER performance than the Flat Rayleigh channel. But, in the Flat Rayleigh channel, the signal is corrupted more severe than in the PedB channel.

From Fig. 12, the throughput performance of AWGN channel is better than the performance of both PedB and Flat Rayleigh chan-

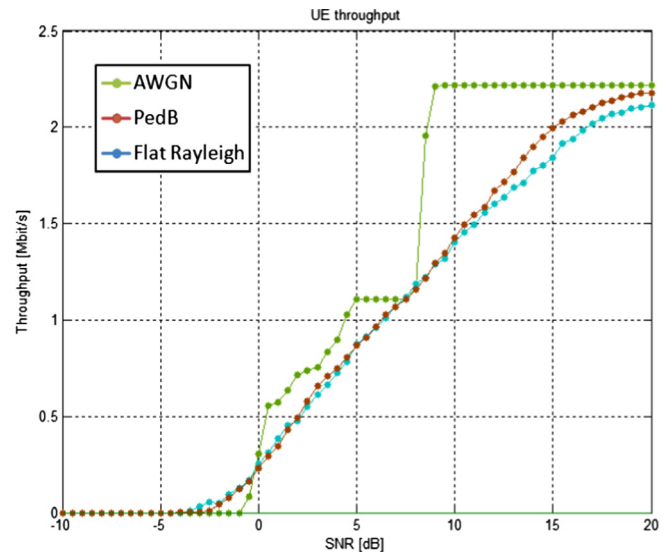


Fig. 12. Throughput vs. SNR for different channel types, SISO.

Table 5

At low channel SNRs, higher CQI feedback values will have poor BER performance than the lower CQI feedback values. However, by increasing the signal power, lower error ratio for higher CQI feedback values can be achieved. In Fig. 10, the throughput performance for different CQI configurations and different modulation schemes associated with different ECRs can be obtained. The higher CQI values result in better overall throughput performance but at the price of higher channel SNR.

CQI	Modulation	ECR
1	4QAM	0.0762
2	4QAM	0.1172
3	4QAM	0.1885
4	4QAM	0.3008
5	4QAM	0.4385
6	4QAM	0.5879
7	16QAM	0.3691
8	16QAM	0.4785
9	16QAM	0.6016
10	64QAM	0.4551
11	64QAM	0.5537
12	64QAM	0.6504
13	64QAM	0.7539
14	64QAM	0.8525
15	64QAM	0.9258

nels. This channel results in throughput improvement to higher than 2 Mbit/s at the channel SNR = 8 dB; however, the throughput of the system experiencing PedB or Flat Rayleigh channels can be improved to higher than 2 Mbit/s at the SNR = 20 dB, which is 12 dB higher than that of AWGN channel.

### 5.2.3. Performance analysis for different turbo code iterations

The BER and BLER performances are shown in Figs. 13 and 14 respectively. At turbo decoder, data decoding function is iterated until the decoder maximum iteration number is reached. After each iteration, the output of turbo decoder is stored and later used as an input parameter for the next decoding iteration helping the decoder to make a better decision. Thus, by increasing the number of turbo decoder iterations the BER performance of the system can be improved, as in Fig. 13 at the 8th iteration, a BER of  $10^{-6}$  can be achieved at the channel SNR = 8 dB.

Fig. 14 illustrates that the SNR improvement gap between 1st and 3rd iterations is much larger than the SNR improvement between 3rd and 5th iterations.

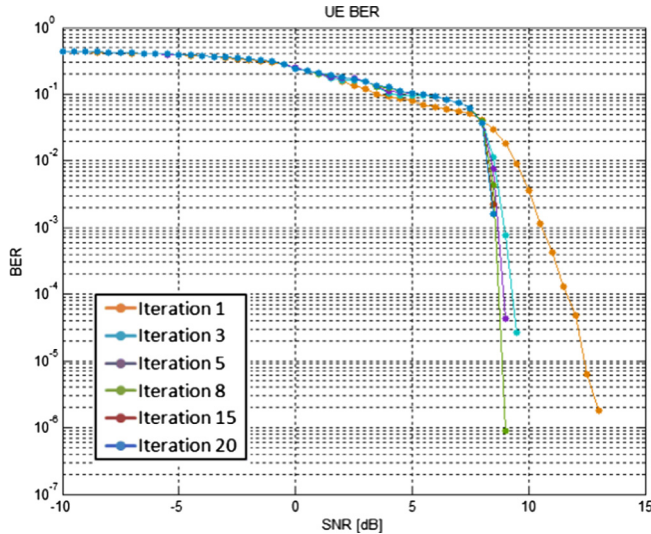


**Fig. 13.** BER vs. SNR for different turbo code iterations, SISO.

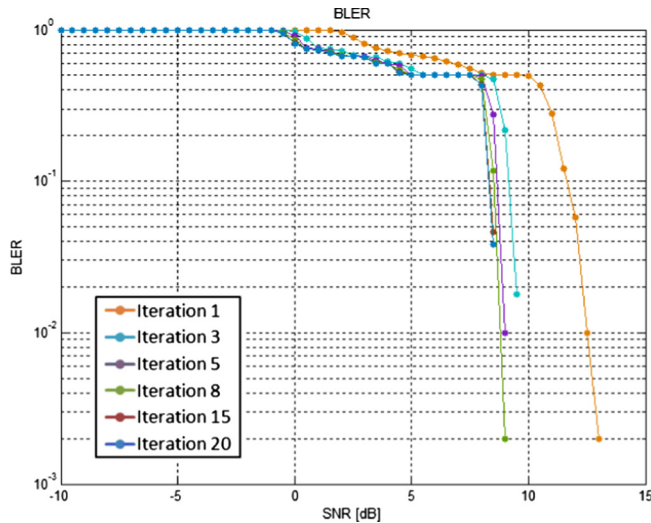


**Fig. 14.** BLER vs. SNR for different turbo code iterations, SISO.

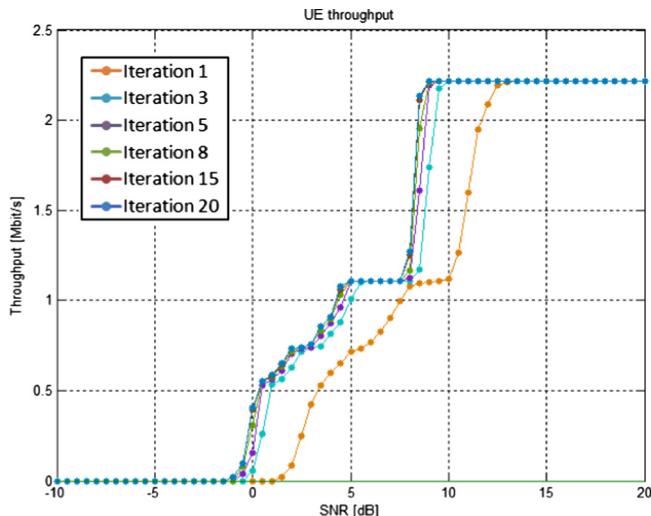


**Fig. 15.** Throughput vs. SNR for different turbo code iterations, SISO.

In [Fig. 15](#) the throughput performance improvement between low iteration numbers is much larger than the throughput performance improvement between high iteration numbers.

#### 5.2.4. Performance analysis of different HARQ retransmissions

From the [Figs. 16 and 17](#), by increasing the number of HARQ retransmissions the system BER and BLER are decreased. This is because when a packet is found to be in error for the first time, up to 3 retransmission requests are sent toward the transmitter while the corrupted packet at the receiver is ignored. For SNR values 0–8 dB the 3 HARQ retransmissions technique improves the system BER performance moderately better than no HARQ retransmissions technique. But, at the expenses of increasing SNR to 9 dB, both methods perform alike. Therefore, there is no point of using HARQ retransmissions technique for high channel SNR values.

In [Fig. 18](#), at low channel SNR values, a significant difference between no HARQ and 3 HARQ retransmission schemes can be seen. This is since the 3 HARQ retransmissions technique can request data retransmissions for up to 3 times.

#### 5.2.5. Performance analysis of different channel estimations

In [Fig. 19](#) the system's BER improvement uses the Perfect or Minimum Mean Square Error (MMSE), with a comparison to the Least Squares (LS). However, in the MMSE channel estimator, it requires the second-order statistics of the channel and the noise, and it makes the MMSE channel estimator much more accurate than the LS. As at the channel SNR of 8 dB, by utilizing the MMSE channel estimator or the Perfect channel estimator a BER close to  $10^{-6}$  can be achieved. However, choosing the LS algorithm as the channel estimator can only give a BER close to  $10^{-6}$  at the expense of a higher channel SNR value which is 10 dB.

[Fig. 20](#) shows the throughput performance of Perfect, MMSE and LS channel estimators, where the SNR improvement of the MMSE channel estimator in comparison to the LS channel estimator is approximately 2 dB. While a system using the MMSE channel estimator performs only about 0.5 dB worse than a system with perfect channel knowledge.

#### 5.2.6. Performance analysis of different user speeds

[Figs. 21 and 22](#) present the BER and throughput performances of the LTE physical layer respectively, while AWGN channel was simulated to associate a fixed user, and PedB and Flat Rayleigh channels associate users with 10 km/h and 100 km/h of velocity

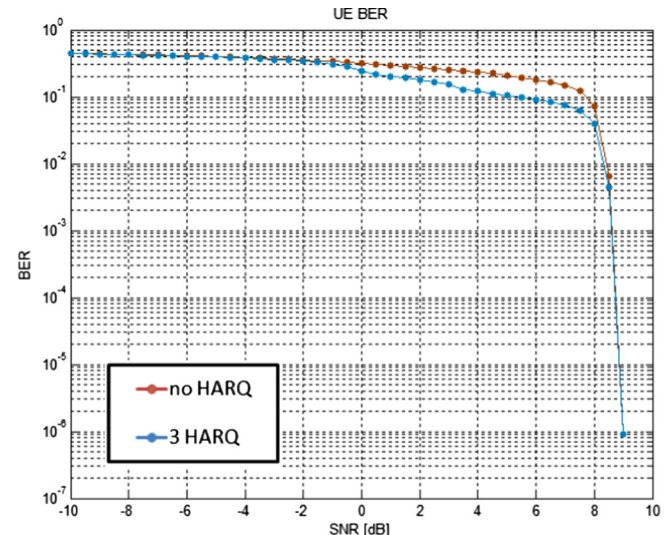


**Fig. 16.** BER vs. SNR for different number of HARQ retransmissions, SISO.

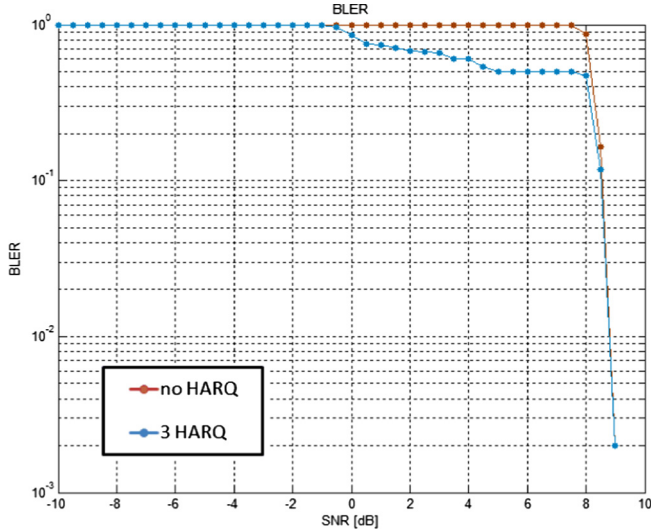


**Fig. 17.** BLER vs. SNR for different number of HARQ retransmissions, SISO.

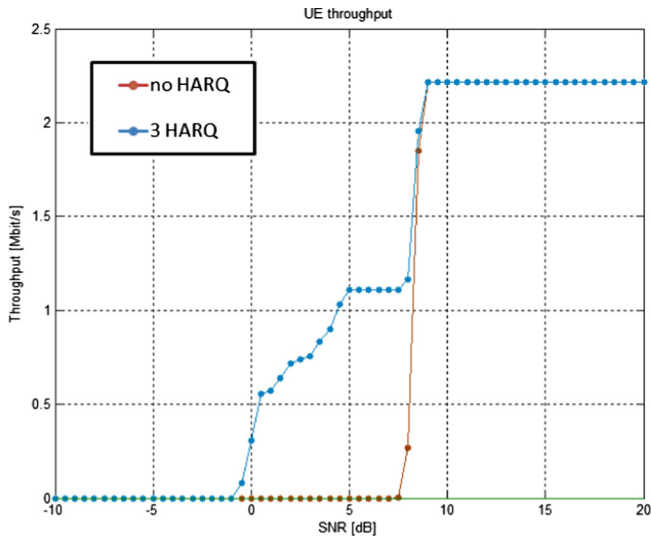


**Fig. 18.** Throughputs vs. SNR for different HARQ retransmissions, SISO.

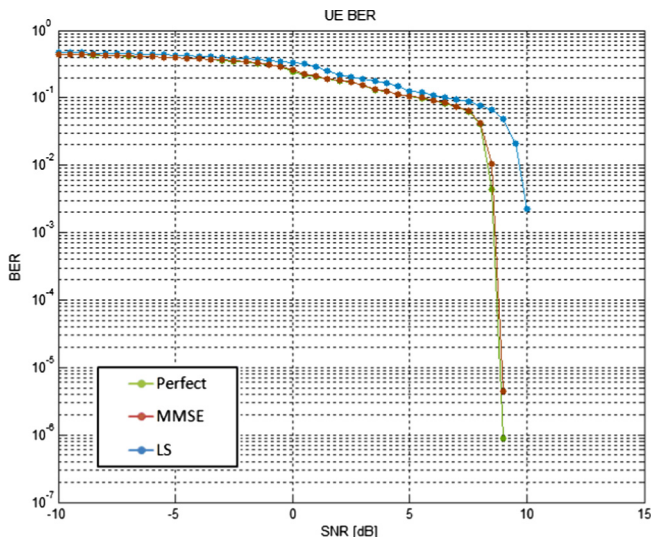


**Fig. 19.** BER vs. SNR for diverse types of channel estimators, SISO.

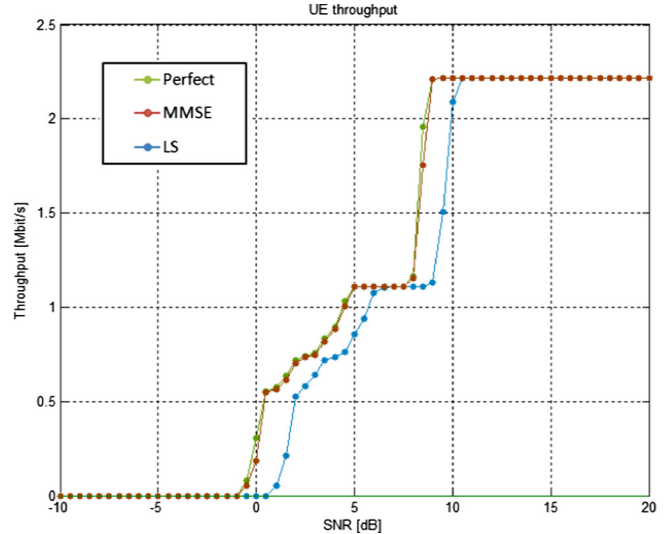


**Fig. 20.** Throughput vs. SNR for diverse types of channel estimators, SISO.

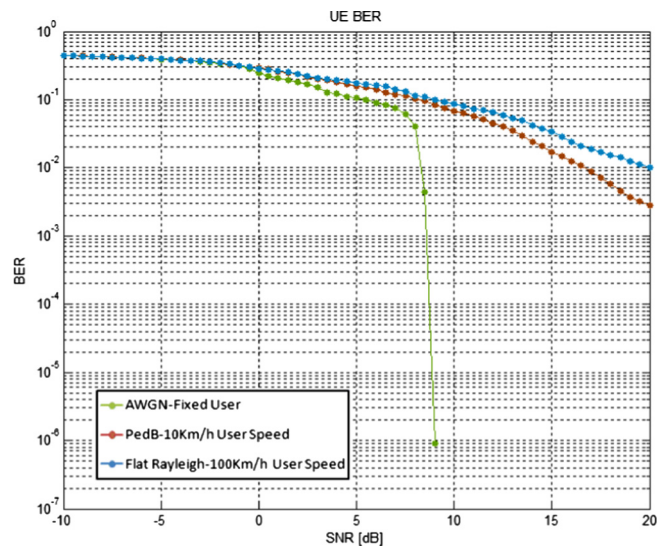


**Fig. 21.** BER vs. SNR for different user speeds, SISO.

respectively. If the SNR is low, the AWGN channel results in the best BER performance. As the UE experiencing this channel condition, we can achieve data with the  $\text{BER} = 10^{-6}$  at the  $\text{SNR} = 8 \text{ dB}$ . While, in case of PedB channel associating a user with 10 km/h velocity, as well as the Flat Rayleigh channel associating a user with 100 km/h velocity, since the UEs experience the small-scale fading channel type (PedB and Flat Rayleigh). Comparing the Figs. 21 and 22 with Figs. 11 and 12, the LTE standard is not sensitive to user mobility and user velocity, as the performances of the channels tested in both with user mobility and without user mobility scenarios are very similar.

### 5.3. MIMO techniques

In LTE, the MIMO technique with the possibility of up to eight transmit antennas and eight receive antennas in downlink, and up to four transmit antennas and four receive antennas in uplink direction are supported. This feature allows transmitting up to eight streams of multi-layer in downlink and up to four multi-layer streams in uplink.

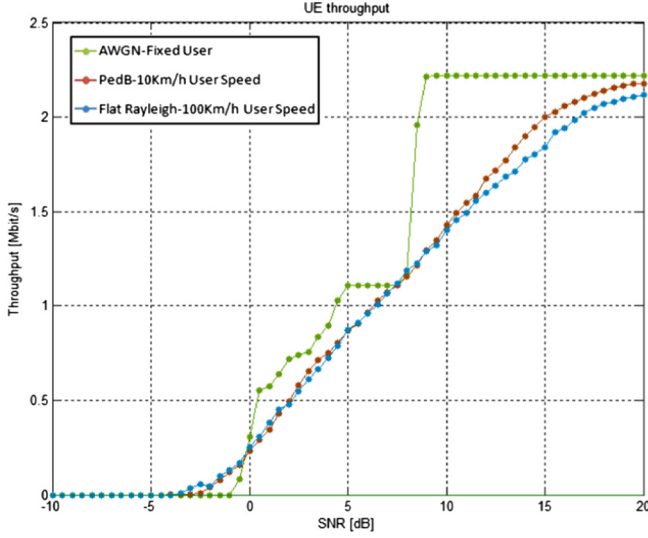


**Fig. 22.** Throughputs vs. SNR for different user speeds, SISO.

### 5.3.1. Performance analysis of different CQI numbers

We analyze the impact of a different number of CQI feedbacks on a MIMO TxD  $4 \times 2$  system in the LTE standard. In Fig. 23, the CQI number results in an increase of required SNR value to help keep the BER value at a desired value. Thus, to achieve a low BER value while increasing the quantity of CQI feedbacks, a penalty of enhancing SNR must be paid. Since higher CQI values indicate higher modulation orders and higher ECRs, thus higher bit rate is transferred, which causes increasing the signal bandwidth and overlapping. So, we see that at low channel SNRs, higher CQI feedback values will have worse BER performances than the lower CQI feedback values.

In Fig. 24, the increasing CQI numbers result in better throughput performance. Since higher CQI feedback numbers indicate higher modulation orders and higher ECRs; hence, higher data rate and thus higher throughput can be achieved, but it requires an increase of signal power. Therefore, a trade-off between higher CQI numbers and lower SNR values should be made to design a desirable system.

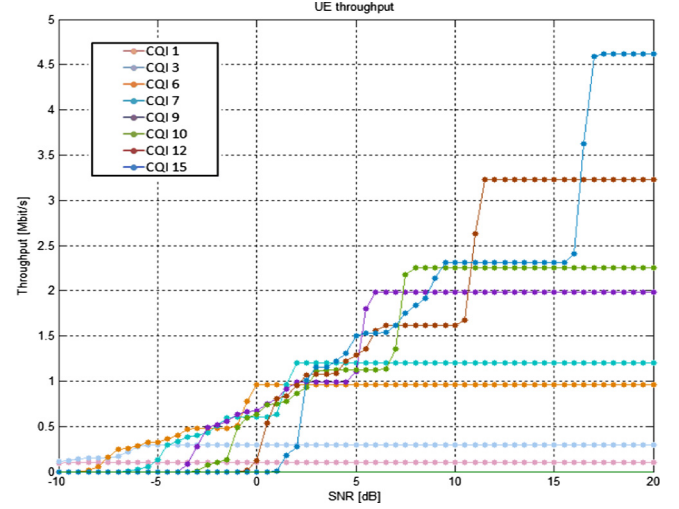


**Fig. 24.** Throughput vs. SNR for different CQIs, MIMO  $4 \times 2$ .

### 5.3.2. Performance analysis of different channel types

In Figs. 25 and 26, BER and BLER performances of four channel types, namely; AWGN, PedB, VehicularB (VehB) and Flat Rayleigh are shown using a MIMO TxD 4x2 technique. If low SNR value is desired, the AWGN channel performs the best among all four channels in terms of error performance. As the system using AWGN channel can approach the  $\text{BER} = 10^{-2}$  at SNR lower than 6 dB. However, PedB, VehB, and Flat Rayleigh channel models which are small-scale fading channel types, perform much worse than the AWGN in terms of the error performance. In Flat Rayleigh channel, the signal is corrupted more severe than in the PedB and VehB channels.

In Fig. 27, AWGN channel type results in better performance in comparison with VehB and Flat Rayleigh channels. The PedB channel has better throughput performance than both the VehB channel and the Flat Rayleigh channel. In the Flat Rayleigh channel, the signal is corrupted more severe than in the PedB and VehB channels, since the Rayleigh fades is added to the Flat fades, and the signal also suffers from Non-Line-of-Sight propagation in multipath fading.

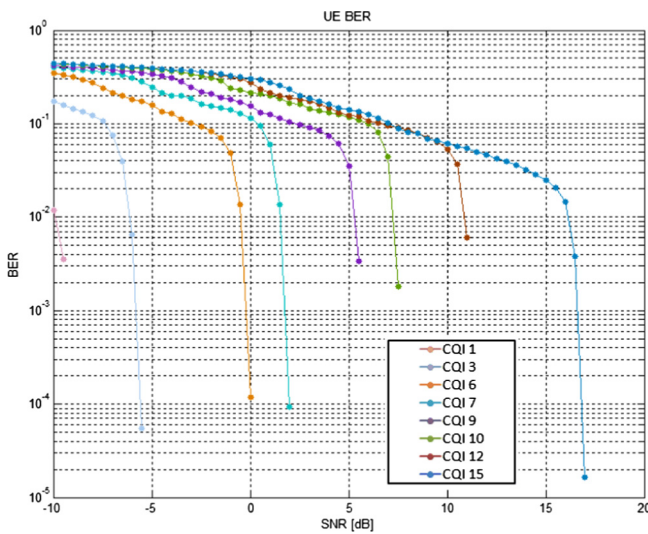


**Fig. 23.** BER vs. SNR for different CQIs, MIMO.

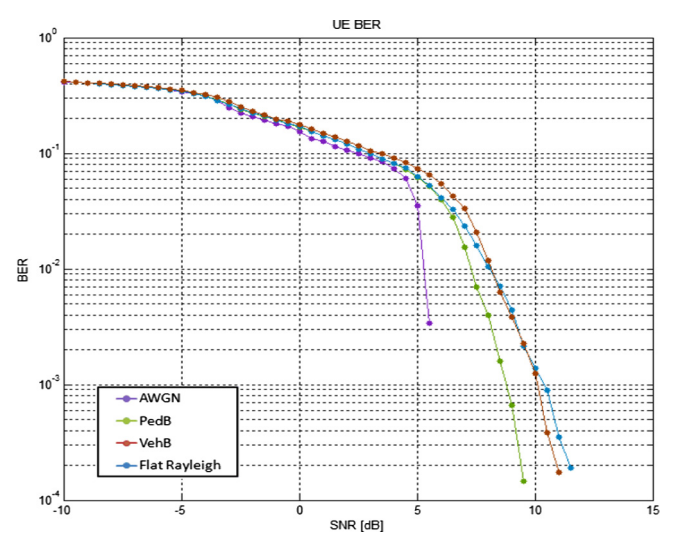


**Fig. 25.** BER vs. SNR for different channel types, MIMO  $4 \times 2$ .

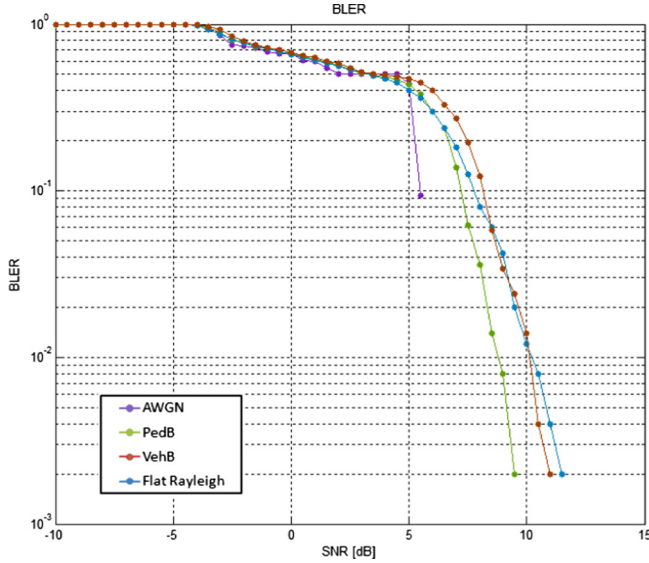


**Fig. 26.** BLER vs. SNR for different channel types, MIMO 4 × 2.

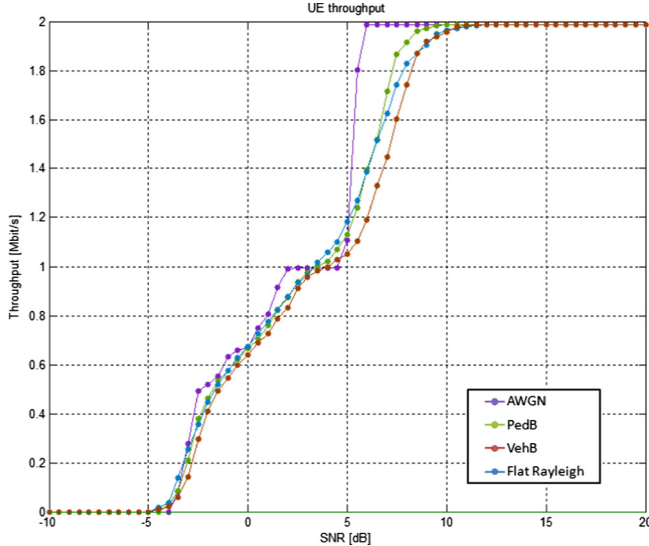


**Fig. 27.** Throughputs vs. SNR for different channel types, MIMO 4 × 2.

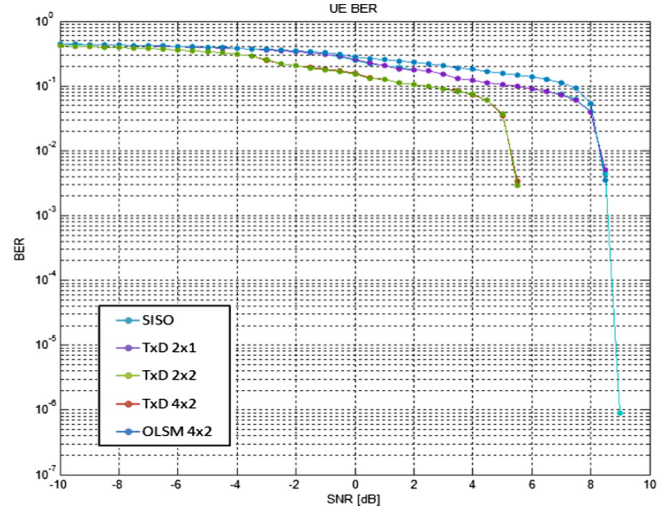


**Fig. 28.** BER vs. SNR for different antenna diversities.

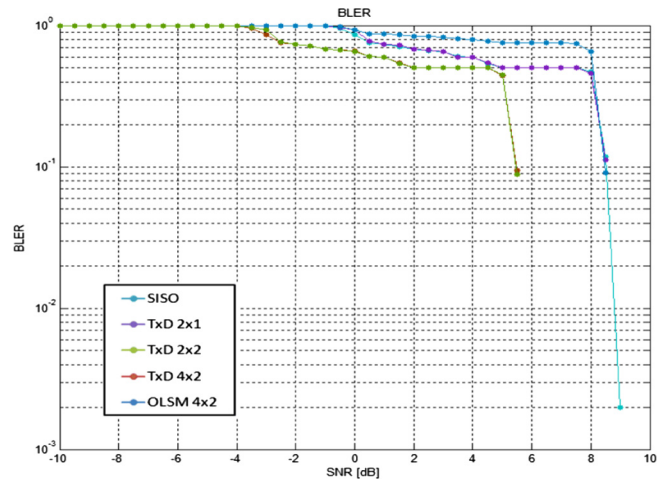


**Fig. 29.** BLER vs. SNR for different antenna diversities.

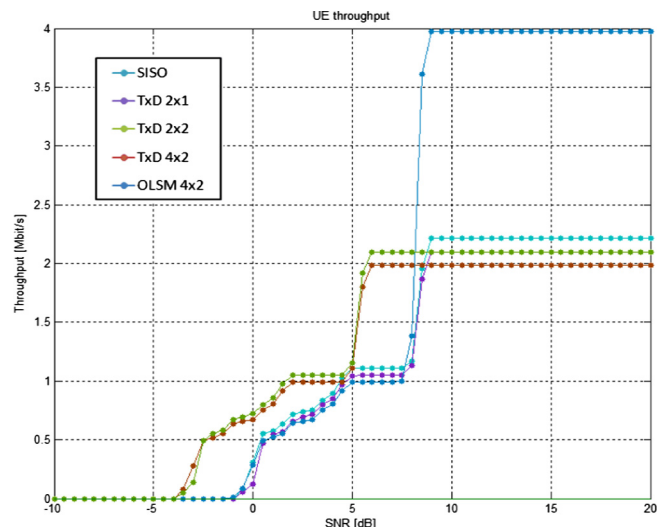


**Fig. 30.** Throughputs vs. SNR for different antenna diversities.

### 5.3.3. Performance analysis of different antenna diversities

In this scenario, BER, BLER and throughput performances of various antenna diversities, namely; SU-SISO, SU-MIMO TxD 2 × 1, SU-MIMO TxD 2 × 2, SU-MIMO TxD 4 × 2 and Open Loop Spatial Multiplexing (OLSM) TxD 4 × 2, used in LTE standard are analyzed. In Figs. 28 and 29, the impact of different antenna diversities on BER and BLER performances of LTE systems are presented, and the BER and BLER improvements in SU-MIMO TxD 2 × 2 and SU-MIMO TxD 4 × 2 techniques in comparison to other SISO and MIMO techniques is significant. As, in the case of the  $\text{BER} = 10^{-2}$  desired, utilizing SU-MIMO TxD 4 × 2 and SU-MIMO TxD 2 × 2 techniques result in 3 dB SNR gain in comparison with other techniques. This improvement is due to the increase of the number of the receive antenna, as when using two receive antenna instead of one the variance of the noise term is scaled by a factor of 2. Figure 28. BER vs. SNR for different antenna diversities.

Fig. 30 shows the system throughput performance and the throughput improvement of OLSM TxD 4x2 system is compared to other systems. This system can enhance the system maximum

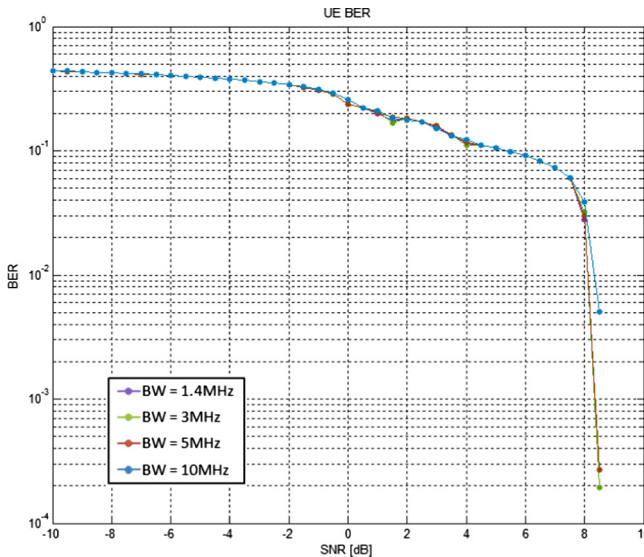


Fig. 31. BER vs. SNR for different channel bandwidths, MIMO 2 × 1.

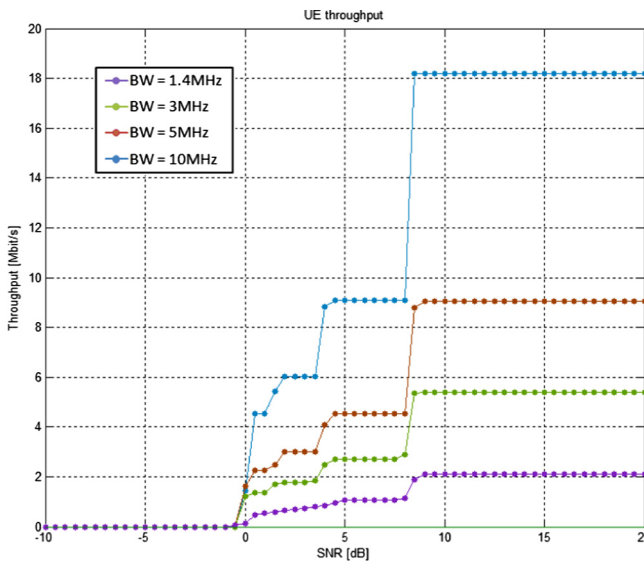


Fig. 32. Throughputs vs. SNR for different channel bandwidths, MIMO 2 × 1.

throughput to approximately twice the maximum throughput of other systems. The maximum throughput achieved by SU-MIMO TxD 4 × 2 technique is lower than the maximum throughput achieved by two SU-MIMO TxD 2x1 and SU-MIMO TxD 2 × 2 techniques.

#### 5.3.4. Performance analysis of different channel bandwidths

In Fig. 31, BER performance of few channel bandwidths (1.4 MHz, 3 MHz, 5 MHz and 10 MHz) on an SU-MIMO TxD 2 × 1 LTE system is presented, where the BER difference between different channel bandwidths is insignificant. This is due to taking the advantage of OFDM technique in downlink transmission, which results in decreasing ISI in high data rates. In addition to OFDM technique, using turbo coding, interleaver, and HARQ retransmissions help to keep the system BER at low levels.

By analyzing Fig. 32, increasing the transmission bandwidth results in increasing the system throughput dramatically. Higher system throughput can be obtained by utilizing larger channel bandwidths in the scenario.

## 6. Conclusion

This study focused on the main parameters of LTE physical layer as well as the most frequent scenarios for mobile communications. Several techniques and technologies such as OFDM, OFDMA, SC-FDMA, and MIMO for the cellular systems were studied using a Link Level Simulator based on MATLAB program.

A reduction of system BER and BLER can be achieved in LTE downlink transmission. The effects of different numbers of HARQ retransmissions and turbo code iterations were investigated for SISO mode. Different user speeds were simulated and analyzed in terms of BER, BLER, and throughput in SISO systems, where MMSE channel estimator has a much better consequence on transmission than the LS channel estimator. A system experiencing AWGN channel condition results in a significant BER and throughput improvement compared to systems involving with PedB, VehB or Flat Rayleigh channel types. The system involving with PedB channel results in a better performance. In MIMO systems, increasing the system bandwidth is a very effective way, but this solution obviously is significantly costly for service providers. Moreover, evaluation of physical layer throughput can be performed for next Release(s) of 3GPP, since some effective modern technologies such as bandwidth extension up to 100 MHz and supporting more antenna ports can highly impact the performance.

## References

- [1] X. Hou, B. Lin, R. He, X. Wang, Infrastructure planning and topology optimization for reliable mobile big data transmission under cloud radio access networks, *EURASIP J. Wireless Commun. Netw.* 2016 (2016) 1.
- [2] C.-C. Yang, J.-Y. Chen, Y.-T. Mai, C.-H. Liang, Adaptive load-based and channel-aware power saving for non-real-time traffic in LTE, *EURASIP J. Wireless Commun. Netw.* 2015 (2015) 1.
- [3] R.-R. Su, I.-S. Hwang, B.-J. Hwang, A new cross-layer scheme that combines grey relational analysis with multiple attributes and knapsack algorithms for WiMAX uplink bandwidth allocation, *EURASIP J. Wireless Commun. Netw.* 2016 (2016) 170.
- [4] D. Tsolka, E. Lioutou, N. Passas, L. Merakos, Lte-a access, core, and protocol architecture for d2d communication, in: *Smart Device to Smart Device Communication*, ed: Springer, 2014, pp. 23–40.
- [5] S. Sesia, I. Toufik, and M. Baker, "LTE-The UMTS Long Term Evolution," From Theory to Practice, published in, 2009.
- [6] V.G. Nguyen, Y. Kim, Proposal and evaluation of SDN-based mobile packet core networks, *EURASIP J. Wireless Commun. Netw.* 2015 (2015) 1–18.
- [7] M. Pelcat, Rapid Prototyping and Dataflow-Based Code Generation for the 3GPP LTE eNodeB Physical Layer Mapped onto Multi-Core DSPs, UEB – Université européenne de Bretagne, 2011.
- [8] 3GPP, TS 36.201 Evolved Universal Terrestrial Radio Access (E-UTRA); LTE physical layer; General description, ed, 2010.
- [9] M. Matthe, L.L. Mendes, I. Gaspar, N. Michailow, D. Zhang, G. Fettweis, Multi-user time-reversal STC-GFDMA for future wireless networks, *EURASIP J. Wireless Commun. Netw.* 2015 (2015) 1.
- [10] L. Militano, M. Condoluci, G. Araniti, A. Molinaro, A. Iera, G.-M. Muntean, Single frequency-based device-to-device-enhanced video delivery for evolved multimedia broadcast and multicast services, *IEEE Trans. Broadcast.* 61 (2015) 263–278.
- [11] R.-H. Hwang, C.-F. Huang, C.-H. Lin, C.-Y. Chung, Context-aware multimedia broadcast and multicast service area planning in 4G networks, *Comput. Commun.* 64 (2015) 33–43.
- [12] O.-S. Shin, S.E. Elayoubi, Y.K. Jeong, Y. Shin, Advanced technologies for LTE advanced, *EURASIP J. Wireless Commun. Netw.* 2013 (2013) 1.
- [13] 3GPP, "TS 36.211 Evolved Universal Terrestrial Radio Access (E-UTRA); Physical channels and modulation," ed, 2011.
- [14] 3GPP, TS 36.212 Evolved Universal Terrestrial Radio Access (E-UTRA); Multiplexing and channel coding (Release 10), ed, 2011.
- [15] C. Melihfuehrer, M. Wurlich, J. C. Ikuno, D. Bosanska, M. Rupp, Simulating the long term evolution physical layer, presented at the 17th European Signal Processing Conference (EUSIPCO 2009), 2009.
- [16] X. Ling, Y. Chen, Z. Yu, S. Chen, X. Wang, G. Liang, MACRON: The NoC-Based Many-Core Parallel Processing Platform and Its Applications in 4G Communication Systems, in: 2015 23rd Euromicro International Conference on Parallel, Distributed, and Network-Based Processing, 2015, pp. 396–403.
- [17] G. Mohamed, S. El-Rabaei, Service Enhancement for User Equipments in LTE-A Downlink Physical Layer Network, *Wireless Pers. Commun.* 83 (2015) 149–161.
- [18] D. Martín-Sacristán, J.F. Monserrat, J. Cabrejas-Penuelas, D. Calabuig, S. Garrigas, N. Cardona, On the way towards fourth-generation mobile: 3GPP LTE and LTE-advanced, *EURASIP J. Wireless Commun. Netw.*, p. 4, 2009.

- [19] E. Virtej, M. Kuusela, E. Tuomaala, System performance of Single-User MIMO in LTE downlink, Personal, Indoor and Mobile Radio Communications, 2008. PIMRC 2008. IEEE 19th International Symposium on pp. 1–5, 2008.
- [20] J.J. Sanchez, D. Morales-Jiménez, G. Gómez, J. Enbrambasaguas, Physical layer performance of long term evolution cellular technology, Mobile and Wireless Communications Summit, IEEE 16th IST pp. 1–5, 2007.
- [21] K. Beh, A. Doufexi, S. Armour, On the performance of SU-MIMO and MU-MIMO in 3GPP LTE downlink, 2010, pp. 1482–1486.
- [22] 3GPP, R1-072578 Summary of Downlink Performance Evaluation, ed, 2007.
- [23] A. Van Zelst, T.C.W. Schenk, Implementation of a MIMO OFDM-based wireless LAN system, *Signal Proc., IEEE Trans.* 52 (2004) 483–494.
- [24] N. Wei, MIMO Techniques for UTRA Long Term Evolution, Aalborg University, 2007.
- [25] 3GPP, TS 36.101 Evolved Universal Terrestrial Radio Access (E-UTRA); User Equipment (UE) radio transmission and reception (Release 10), ed, 2011.
- [26] 3GPP, TS 36.104 Evolved Universal Terrestrial Radio Access (E-UTRA); Base Station (BS) radio transmission and reception (Release 10), ed, 2011.